Environmental Science & Technology

Article

Cite This: Environ. Sci. Technol. 2018, 52, 13708−13717

pubs.acs.org/est

# Coupling High-Frequency Stream Metabolism and Nutrient Monitoring to Explore Biogeochemical Controls on Downstream Nitrate Delivery

Helen P. Jarvie,*[,†] Andrew N. Sharpley,[‡] Timothy Kresse,[§] Phillip D. Hays,[∥] Richard J. Williams,[†] Stephen M. King,[⊥] and Lawrence G. Berry[‡]

[†]NERC Centre for Ecology and Hydrology, Wallingford, OX10 8BB, United Kingdom

[‡]Department of Crop Soil and Environmental Sciences, University of Arkansas, Fayetteville, Arkansas 72701, United States

[§]U.S. Geological Survey, Lower Mississippi-Gulf Water Science Center, 401 Hardin Road, Little Rock, Arkansas 72211, United States

[∥]U.S. Geological Survey, Lower Mississippi-Gulf Water Science Center/University of Arkansas, Department of Geosciences, 216 Gearhart Hall, Fayetteville, Arkansas 72701, United States

[⊥]STFC Rutherford Appleton Laboratory, Harwell Campus, Didcot, Oxfordshire OX11 0QX, United Kingdom

Supporting Information

**ABSTRACT:** Instream biogeochemical process measurements are often short-term and localized. Here we use in situ sensors to quantify the net effects of biogeochemical processes on seasonal patterns in baseflow nitrate retention at the river-reach scale. Dual-station high-frequency in situ nitrate measurements, were coupled with high-frequency measurements of stream metabolism and dissolved inorganic carbon, in a tributary of the Buffalo National River, Arkansas. Nitrate assimilation was calculated from net primary production, and combined with mass-balance measurements, to estimate net nitrification and denitrification. The combined net effects of these instream processes (assimilation, denitrification, and nitrification) removed >30−90% of the baseflow nitrate load along a 6.5 km reach. Assimilation of nitrate by photoautotrophs during spring and early summer was buffered by net nitrification. Net nitrification peaked during the spring. After midsummer, there was a pronounced switch from assimilatory nitrate uptake to denitrification. There was clear synchronicity between the switch from nitrate assimilation to denitrification, a reduction in river baseflows, and a shift in stream metabolism from autotrophy to heterotrophy. The results show how instream nitrate retention and downstream delivery is driven by seasonal shifts in metabolic pathways; and how continuous in situ stream sensor networks offer new opportunities for quantifying the role of stream biota in the dynamics, fate, and transport of nitrogen in fluvial systems.

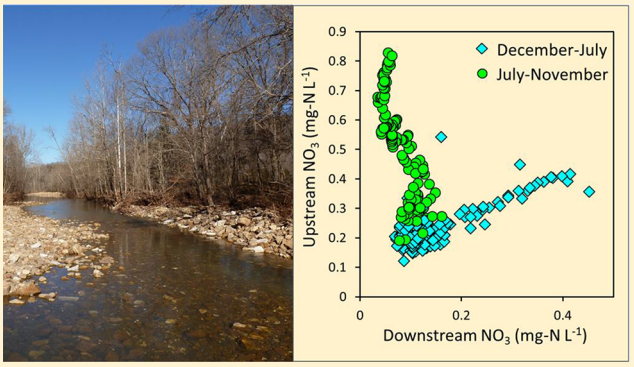




## 1. INTRODUCTION

Nutrients, including nitrogen (N), phosphorus (P), and carbon (C) from agriculture and domestic wastewater, are a major source of water-quality impairment.[1] Excessive nutrient inputs to rivers, streams, and lakes can accelerate growth of nuisance and harmful algae. Resulting increases in microbial activity and depletion of dissolved oxygen (DO) have profound negative consequences for invertebrates and fish, potable water supply, and recreation.[2,3] However, biogeochemical processes in streams also play an important role in regulating downstream nutrient transport, with stream biota retaining and removing nutrients from the water column, reducing downstream ecological impacts.[4−6]

Streams can provide a major sink for nitrate ($NO_3^-$) through uptake (assimilation) by primary production and through denitrification.[7,8] The effectiveness of these processes varies throughout the year and between streams, but conventional methods for estimating $NO_3^-$ uptake are based on relatively few, short-term experimental nutrient additions and isotope measurements,[9−11] making results difficult to extrapolate in space and time.[12] Continuous high-frequency in situ measurements offer new opportunities to explore $NO_3^-$ source dynamics,[13−17] and instream processes have been inferred from single-station diurnal concentration cycles,[12,18,19] longitudinal profiling,[20−23] and nested sensor networks.[24]

Received: June 6, 2018
Revised: October 23, 2018
Accepted: October 30, 2018
Published: October 30, 2018




DOI: 10.1021/acs.est.8b03074
Environ. Sci. Technol. 2018, 52, 13708−13717

In this study, we used in situ sensors to quantify the net effects of biogeochemical processes on seasonal patterns in baseflow $NO_3^-$ retention at the river-reach scale. The approach employed here is novel because it combines dual-station high-frequency $NO_3^-$ measurements, with high-frequency measurements of stream metabolism (analysis of diurnal DO curves to calculate primary production and respiration), dissolved inorganic carbon (DIC), and excess partial pressure of carbon dioxide ($EpCO_2$), to explore the capacity of instream biogeochemical processes to retain and remove $NO_3^-$. High-frequency in situ monitoring of water chemistry and streamflow was undertaken along a 6.5 km experimental reach of Big Creek, a tributary of the Buffalo National Scenic River, Arkansas, U.S.A, and were used to calculate a $NO_3^-$ mass balance along the reach. Net primary production was used to calculate $NO_3^-$ assimilation by photoautotrophs. Daily $NO_3^-$ removal rates and rates of $NO_3^-$ assimilation by photoautotrophs were used to calculate net nitrification and denitrification. The biogeochemical controls on $NO_3^-$ removal were then evaluated in relation to wider ecosystem drivers including streamflow, DO, and stream ecological function, to explore how seasonal shifts in metabolic pathways influence instream $NO_3^-$ retention and downstream $NO_3^-$ delivery.

## 2. MATERIALS AND METHODS

**2.1. Site Description and Water-Quality Monitoring.** Big Creek, a tributary of the Buffalo National Scenic River, Arkansas (Figure 1), is the subject of detailed water-quality monitoring because of a permitted swine concentrated animal feeding operation (CAFO) within the watershed, in operation since September 2013. The Big Creek watershed lies in the karst terrain of the Ozark Plateau of the midcontinental U.S.A. (Figure 1). The watershed area is 236 $km^2$, with 79% of the land area deciduous forest, 3% evergreen forest, 14% grassland/pasture, and 3% developed land (see Supporting Information, SI, S1.1). Swine-manure slurry from the CAFO has been land applied to permitted fields since January 1, 2014, in accordance with State regulations.

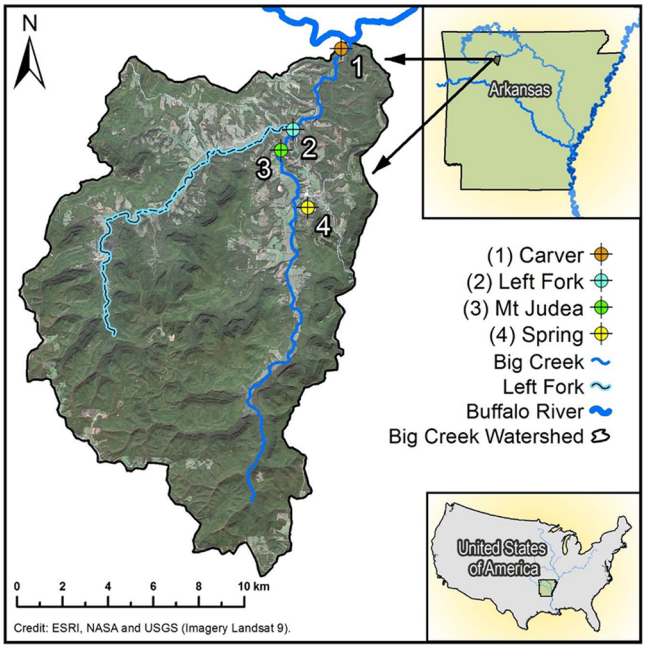


**Figure 1.** Map of the Big Creek watershed and its location.

The focus of this study is an experimental reach of Big Creek, downstream of the CAFO, from an upstream monitoring station at Mt Judea (USGS site 07055790; watershed area 106 $km^2$) to a downstream monitoring station at Carver (USGS site 07055814; watershed area 233 $km^2$), 7.21 and 0.69 km from the confluence between Big Creek and the Buffalo River, respectively (Figure 1). One tributary (Left Fork) enters Big Creek between Mt Judea and Carver. The watershed is a mantled karst terrain characterized by intimate connection between groundwater and surface water; transport of surface-derived nutrients can be rapid[25] (see S1.2).

USGS conducted high-frequency (15 min) $NO_3^-$ monitoring using submersible ultraviolet nitrate probes at Carver (06/03/2014 to 04/29/2017) and Mt Judea (11/01/2014 to 11/01/2015); there was therefore one year of overlapping data (11/01/2014 to 11/01/2015), during which $NO_3^-$ monitoring was undertaken at both Mt Judea and Carver. A water-quality sonde (YSI 6600) operating at Carver simultaneously collected 15 min interval DO, pH, specific conductance, and water temperature data. Further information about the high-frequency water-quality monitoring is provided in S1.3.

Water-quality samples, collected on a weekly basis since 09/12/2013, with additional opportunistic high-flow sampling, at Mt Judea, Left Fork and at a groundwater (spring) monitoring site (Figure 1), provided $NO_3^-$ (by ion chromatography, Dionex ICS-1600); alkalinity (by fixed-end point acidimetric titration to pH 4.5[26]); and conductivity (VWR Symphony B10C) data. All nitrate concentrations are reported as $NO_3$–N (mg-N $L^{-1}$). Water-quality data are available at https://bigcreekresearch.org/.

**2.2. Stream-Flow Measurements and Hydrograph Separation.** Stream flow was measured using established USGS streamflow gauging methods[27] (see S1.4). A two-component mixing model was used to partition the contributions to streamflow from groundwater and surface runoff,[28] using alkalinity as a conservative groundwater tracer (see S1.5).

**2.3. Analysis of Diurnal Dissolved Oxygen Curves to Calculate Primary Production and Respiration.** The daily average gross primary production, daily average ecosystem respiration and reaeration coefficient were calculated from the series of diurnal DO curves at Carver (see S1.6), using a piecewise solution of the mass balance, DO model[29] simplified for the situation where the deficit does not vary spatially (eq 1): the Delta method.[30,31]

$$dD/dt + k_a D = ER_{av} - GPP_{av}(t) \quad (1)$$

where $D$ is the DO deficit (mg-$O_2$ $L^{-1}$), $t$ is the time (days), $k_a$ is the reaeration coefficient, $ER_{av}$ is the ecosystem respiration (mg-$O_2$ $L^{-1}$ $d^{-1}$), and $GPP_{av}$ is the gross primary production (mg-$O_2$ $L^{-1}$ $d^{-1}$); these are standard measures of ecosystem respiration and gross primary production in river systems.[32]

Odum[33] suggested a classification system of flowing-water communities based on oxygen metabolism by using the ratio of $GPP_{av}$ to $ER_{av}$ (GPP/ER). Respiration is associated with both plant and microbial activity. Photosynthesis is only associated with plants. Autotroph-dominated communities are represented by GPP/ER values >1, whereas heterotroph-dominated communities are represented by GPP/ER values <1.

**2.4. Use of the THINCARB Model for Calculating Dissolved Inorganic Carbon Concentrations and Excess**


DOI: 10.1021/acs.est.8b03074
Environ. Sci. Technol. 2018, 52, 13708−13717

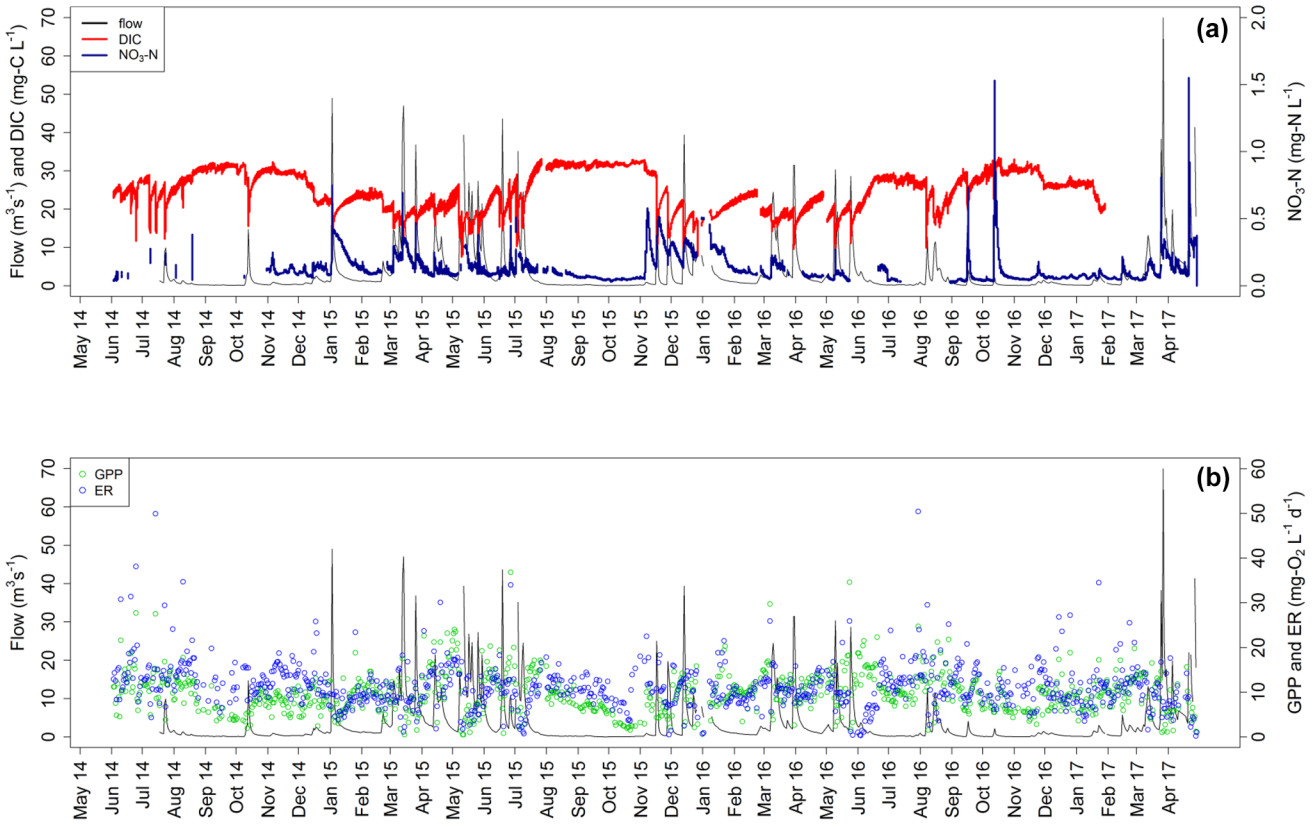


**Figure 2.** Time series at the downstream monitoring site (Carver), from May 2014 to May 2017, showing: (a) nitrate ($NO_3$–N), dissolved inorganic carbon (DIC) and streamflow; and (b) daily average gross primary production (GPP), ecosystem respiration (ER), and streamflow.

**Partial Pressure of Carbon Dioxide.** The THINCARB model (THermodynamic modeling of INorganic CARBon)[34] uses pH, Gran Alkalinity ($Alk_{Gran}$) and temperature measurements to calculate dissolved inorganic carbon (DIC) concentrations and DIC speciation from the excess partial pressures of carbon dioxide ($EpCO_2$) in freshwaters. THINCARB is open access and is described in detail in Jarvie et al. (2017);[34] an outline is provided in S1.7. Prior to use, alkalinity measurements in units of mg-$CaCO_3$ $L^{-1}$ were first converted to $Alk_{Gran}$ (in $\mu$eq $L^{-1}$), where 1 mg $L^{-1}$ $CaCO_3$ = 19.98 $\mu$eq $L^{-1}$.[34]

THINCARB was applied to the high-frequency sonde data from Carver. Specific conductance was used as a surrogate for alkalinity: using the regression relationship between $Alk_{Gran}$ and specific conductance ($\kappa$), measured across the Big Creek watershed, including the spring, and Mt Judea, Left Fork, and Carver stream sites: $Alk_{Gran}$ = 8.65 (±0.28) × $\kappa$ − 6.44 (±66), $R^2$ = 0.95, $n$ = 270, $P$ < 0.001 (numbers in parentheses represent twice the standard error). By applying this regression equation to the hourly $\kappa$ series, an hourly alkalinity record was derived, which was then used alongside the hourly pH and water-temperature data, to calculate a high-frequency DIC and $EpCO_2$ series.

**2.5. Mass-Balance Calculation of Baseflow Nitrate Fluxes, Instream Losses, and Net Nitrification and Denitrification.** Daily mass-balance calculations were undertaken for eight quiescent, low-flow periods (each typically of 1–2 weeks). USGS stream-velocity readings from Carver ranged from 0.457 and 1.22 m $s^{-1}$, and with a stream distance along the experimental reach of 6.52 km, the travel times ranged from 3.96 to 1.48 h. Therefore, daily mass balances over a 24-h period were assumed sufficient to account for transit of $NO_3^-$, given: (a) the relatively short travel times; (b) the high degree of stationarity in flux transfers during quiescent baseflow conditions; and (c) that calculated daily mass balances were averaged over a 1–2 week period.

The 15 min $NO_3^-$ measurements at Mt Judea and Carver were converted to daily means, and daily nitrate loads at each site were calculated using the corresponding gauged daily streamflow data. To account for flow accretion along the reach, the difference between the daily flow downstream at Carver, and the upstream site at Mt Judea was calculated. The increase in flows was assumed to be input from Left Fork (Figure 1).

Daily $NO_3^-$ input loading to the reach ($L_T$) was calculated as the sum of the daily $NO_3^-$ loads from Mt Judea ($L_{MJ}$) and Left Fork ($L_{LF}$):

$$L_T = L_{MJ} + L_{LF} \quad (2)$$

There was no high-resolution $NO_3^-$ monitoring on Left Fork, so weekly $NO_3^-$ measurements from grab samples taken at Left Fork were combined with the measured daily flow accretion to derive daily loads from Left Fork (S1.8.1). A sensitivity analysis evaluated the potential effects of under- or overestimating Left Fork $NO_3^-$ concentrations by ±50% (Tables SI1 and SI2).

Within this karst watershed, some of the flow accretion will arise from direct groundwater input into Big Creek. Discharge data were not available from the Left Fork tributary, and direct apportionment of contributions from Left Fork and groundwater was not possible. We therefore evaluated a second, alternative "endmember" case scenario whereby all of flow


DOI: 10.1021/acs.est.8b03074
Environ. Sci. Technol. 2018, 52, 13708–13717

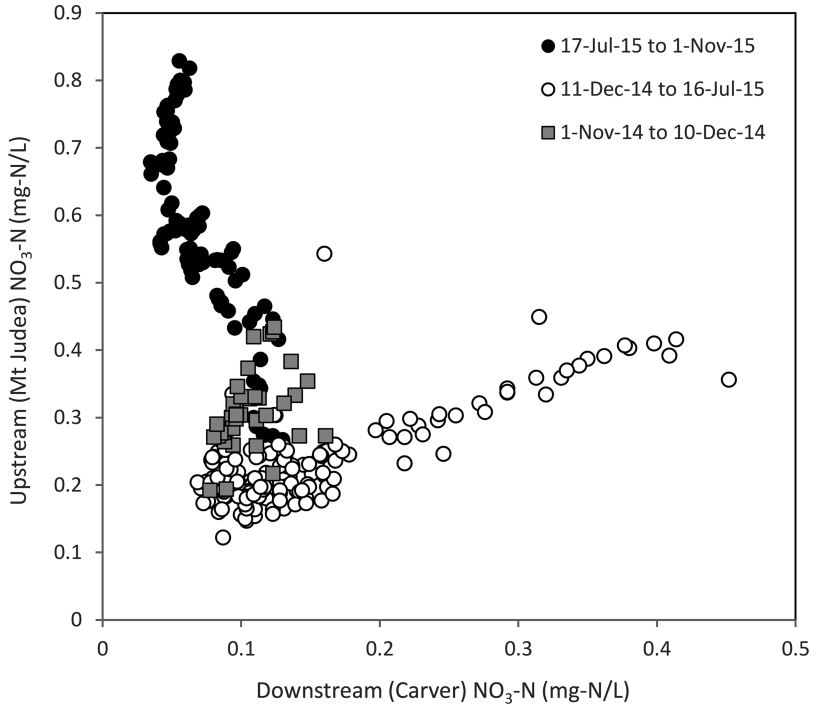


**Figure 3.** Scatter plot showing the relations between mean daily nitrate concentrations upstream at Mt Judea and downstream at Carver.

accretion was attributed to direct groundwater contribution (S1.8.2).

The daily instream $NO_3^-$ load removal ($L_R$) along the reach was calculated as the difference between the daily input $NO_3^-$ loading ($L_T$), and the daily $NO_3^-$ load at Carver ($L_C$):

$$L_R = L_T - L_C \quad (3)$$

To allow direct comparison with rates of assimilatory $NO_3^-$ uptake by photosynthesis, $L_R$ (kg-N $d^{-1}$) was then converted to a daily $NO_3^-$ removal rate, $U_T$ (mg-N $L^{-1}$ $d^{-1}$). $U_T$ incorporates both assimilatory $NO_3^-$ uptake by photoautotrophs ($U_A$), heterotrophic $NO_3^-$ removal through direct uptake and denitrification ($U_D$), and $NO_3^-$ enrichment due to remineralization via nitrification ($R$):[20]

$$U_T = U_A + U_D - R \quad (4)$$

$U_A$ was estimated from the $GPP_{av}$ measurements.[12,35] $GPP_{av}$ data were converted into net primary production (NPP), assuming that autotrophic respiration consumed 50% of the $GPP_{av}$.[36,37] NPP data were then converted from units of $O_2$ uptake (mg-$O_2$ $L^{-1}$ $d^{-1}$) to C uptake (mg-C $L^{-1}$ $d^{-1}$), with a photosynthetic quotient of 1.00, then converted to $NO_3^-$ uptake (mg-N $L^{-1}$ $d^{-1}$), using a molar ratio of C:N of 12.[38] Subtracting $U_T$ from $U_A$ provides a measure of either net nitrification (positive values) or net heterotrophic $NO_3^-$ removal through direct uptake and denitrification, hereafter referred to as "net denitrification" (negative values). When the river was influent, loss of $NO_3^-$ to groundwater was accounted for, as described in S1.8.3.

## 3. RESULTS AND DISCUSSION

**3.1. Three-Year Time Series of Nitrate, Dissolved Inorganic Carbon and Stream Metabolism.** The hourly $NO_3^-$ and DIC concentrations variations at Carver were driven by streamflow, but in opposing directions (Figure 2a). The mean and median $NO_3^-$ concentrations were 0.128 and 0.093 mg-N $L^{-1}$, respectively. Nitrate concentrations at Carver were lowest during baseflow (mean 0.043 mg-N $L^{-1}$; lowest 10% of flows) and highest during storm runoff (mean 0.278 mg-N $L^{-1}$; highest 10% of flows), arising from nonpoint-source mobilization and delivery of $NO_3^-$ during rainfall events.

The mean and median DIC concentrations were 24.8 and 25.2 mg-C $L^{-1}$, respectively. DIC concentrations were highest during baseflow (mean 31.7 mg-C $L^{-1}$), with DIC concentrations diluted by storm runoff (mean 13.2 mg-C $L^{-1}$). Highest DIC and lowest $NO_3^-$ concentrations occurred during the extended low-flows between August and November 2015.

The mean and median molar C:N ratios were 356 and 305, respectively. The mean C:N ratio during baseflow was 882, and 82 during stormflow. C:N ratios greater than ~6.6 are indicative of stoichiometric depletion of N relative to C.[39] Absolute $NO_3^-$ concentrations below ~0.1 mg-N $L^{-1}$ are deemed likely to be limiting to algae, with algal growth response to $NO_3^-$ enrichment occurring between 0.38 to 1.79 mg-N $L^{-1}$.[40] Therefore, under average and baseflow conditions at Carver, a clear potential exists for algal growth to be limited by low $NO_3^-$ availability.

No longer-term trends in either $NO_3^-$ or DIC were observed over the three years. These high-frequency monitoring results are consistent with results from near-weekly water-quality monitoring of Big Creek at Mt Judea, which showed no statistically significant increasing or decreasing trends in dissolved or particulate forms of P and N concentrations since 2013.[41]

Earlier studies[6] have shown that Ozark streams can be very effective at retaining available nutrients, and buffering additional nutrient inputs. Therefore, the absence of any increasing trend in nutrients in the water column may result from the rapid and efficient uptake of nutrient inputs by stream biota. Consequently, high-resolution stream metabolism and nutrient measurements were used here to detect whether increased photosynthesis or respiration rates resulted from increased


DOI: 10.1021/acs.est.8b03074
Environ. Sci. Technol. 2018, 52, 13708−13717

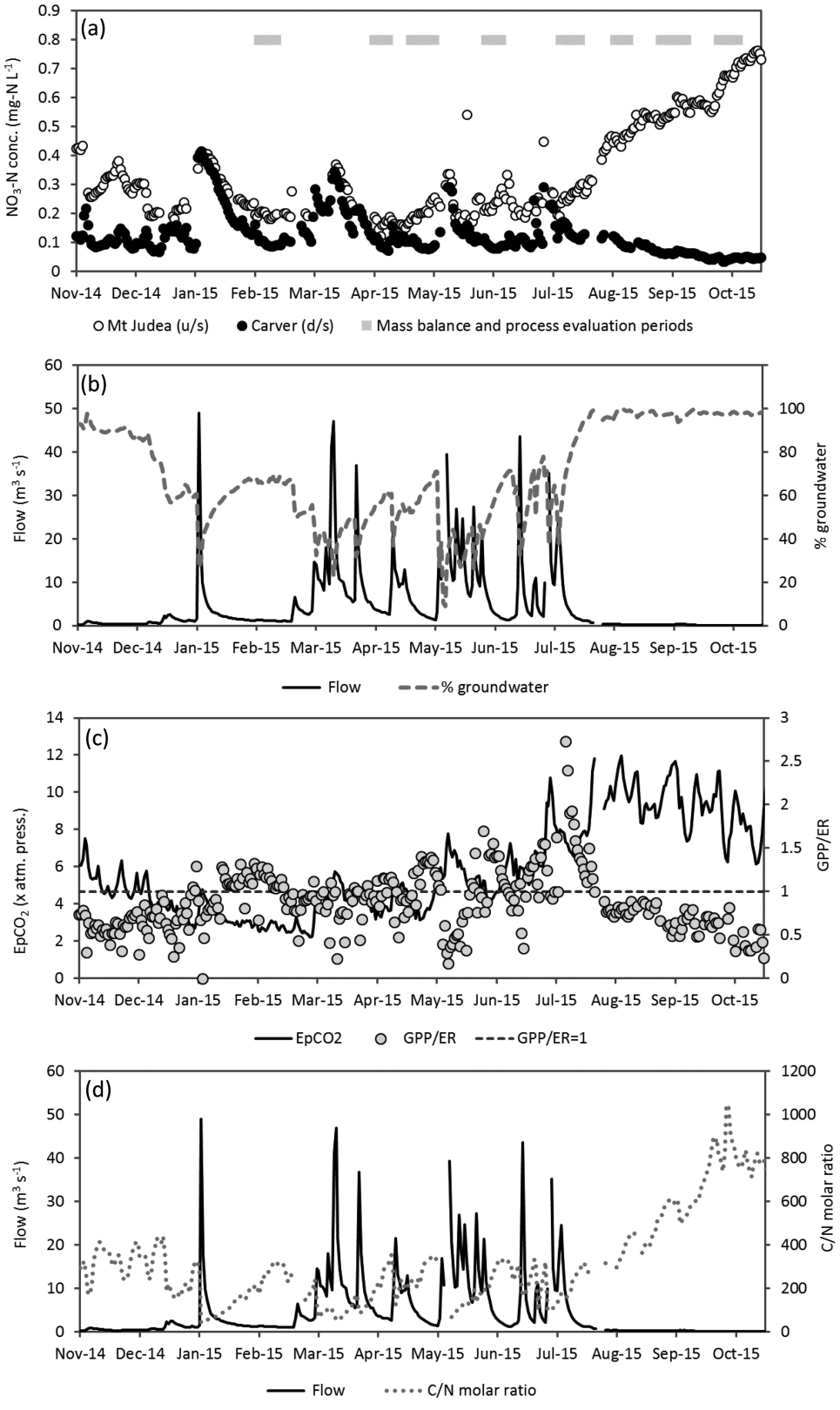


**Figure 4.** Time series from 1 November 2014 to 1 November 2015, showing: (a) Nitrate concentrations upstream at Mt Judea and downstream at Carver, and the lower-flow time periods used for mass balance calculation and evaluation of biogeochemical processes; (b) streamflow at Carver and the percentage groundwater contribution to streamflow; (c) daily ratio of gross primary production: ecosystem respiration (GPP/ER) downstream at Carver (horizontal dashed line shows GPP/ER of 1, i.e., balance between heterotrophy and autotrophy), and excess partial pressure of carbon dioxide ($EpCO_2$); and (d) streamflow and the molar C:N ratio (DIC, dissolved inorganic carbon/$NO_3$−N) downstream at Carver.

nutrient assimilation, even where no increases in water-column nutrient concentrations could be observed.

The time series in daily rates of $GPP_{av}$ and $ER_{av}$, at Carver (Figure 2b), showed no definitive long-term trends between



DOI: 10.1021/acs.est.8b03074
Environ. Sci. Technol. 2018, 52, 13708−13717

Table 1. Seasonal Patterns in Mean Daily $NO_3^-$ Input Loadings ($L_T$) to Big Creek, Mean Daily Instream $NO_3^-$ Load Removal ($L_R$) along the 6.5 km Experimental Reach, Under Low-Flow Conditions, and Mean Daily $NO_3^-$ Load Removal As a Percentage of $NO_3^-$ Inputs ($U_E$)[a]

| season | date range | $NO_3^-$ input loading to reach ($L_T$) (kg-N $d^{-1}$) | instream $NO_3^-$ removal along reach ($L_R$) (kg-N $d^{-1}$) | instream $NO_3^-$ removal ($L_R$) as % of $NO_3^-$ input loading ($L_T$) ($U_E$) |
|---|---|---|---|---|
| winter | 4–13 Feb 2015 | 17.3 (1.12) | 7.68 (0.46) | 44.7 (4.09) |
| spring 1 | 5–12 Apr 2015 | 44.1 (6.35) | 19.0 (2.82) | 43.9 (9.53) |
| spring 2 | 24 Apr–5 May 2015 | 37.9 (15.3) | 16.9 (3.85) | 47.6 (8.93) |
| early summer | 2–10 Jun 2015 | 49.2 (23.6) | 24.1 (8.54) | 51.2 (5.34) |
| mid summer | 11–21 Jul 2015 | 61.7 (44.2) | 14.6 (2.82) | 32.1(14.1) |
| late summer | 7–16 Aug 2015 | 7.56 (1.22) | 5.57 (0.59) | 74.2 (4.66) |
| autumn 1 | 1–14 Sept 2015 | 5.81 (1.23) | 4.49 (0.81) | 77.8 (2.39) |
| autumn 2 | 1–11 Oct 2015 | 2.98 (0.29) | 2.82 (0.25) | 94.8 (1.20) |

[a]Standard deviations are shown in parentheses.

2014 and 2017. $GPP_{av}$ declined rapidly in response to major storm runoff events, but typically recovered within a couple of weeks. Highest $GPP_{av}$ tended to occur during quiescent baseflow or recessional streamflow conditions during the summer (May through August). Both $GPP_{av}$ and $ER_{av}$ declined during the autumn (September through December), reflecting reductions in stream biological activity, and $GPP_{av}$ tended to decline at a faster rate than ER. This was particularly apparent during the extended low-flows between August and December 2015, suggesting a decline in primary production relative to microbial activity and a transition from net autotrophic to net heterotrophic stream communities. During winter baseflows (November through January), $ER_{av}$ tended to exceed $GPP_{av}$. During the 3-yr monitoring, no CAFO-related impacts on either stream nutrient concentrations or metabolism are discernible at Carver.

**3.2. Temporal and Spatial Variability in $NO_3^-$ Concentrations, Relative to Other Key Environmental Variables.** Mean daily $NO_3^-$ concentrations varied between baseflow and storm events at Mt Judea and Carver, during the one year of overlapping data (Figure 3). There was a clear differentiation between a higher-flow period characterized by regular storm events from mid-December 2014 to mid-July 2015, and lower-flow conditions from August to November/December 2015 (Figures 3 and 4).

During the higher-flow period, a positive correlation existed between upstream (Mt Judea) and downstream (Carver) $NO_3^-$, with a ratio approaching 1 (Figure 3). During this high-flow period, $NO_3^-$ concentrations at both upstream and downstream sites ranged between ~0.1 and ~0.4 mg-N $L^{-1}$. Time series data show close convergence between upstream and downstream $NO_3^-$ concentrations during storm-event peak concentrations (Figure 4a,b).

Under lower-flow conditions, $NO_3^-$ concentrations were consistently higher upstream than downstream (Figure 3). The increase in $NO_3^-$ concentrations at the upstream site during the summer and autumn 2015 corresponds with reductions in flow. This is typical of the longer-term hydrologically driven cycles in $NO_3^-$ concentrations observed at the upstream site, reflecting a strong flow dependency, with highest concentrations under the lowest flows, and dilution with increasing flow (Figure SI1a,b,c). The strong increase in $NO_3^-$ concentrations during July to November 2015 therefore reflects hydrological controls, and is consistent with falling flows. The high $NO_3^-$ concentrations in autumn 2015 subsequently declined with the onset of higher flows (Figure SI1a,b).

The gap in $NO_3^-$ concentrations between upstream and downstream sites widened with decreasing flow, particularly during the protracted low-flows between mid-July and November 2015. During this time, minimal soil water contributed to streamflow, and almost all (>95%) of streamflow was derived from groundwater (Figure 4a,b). By the end of October 2015, upstream $NO_3^-$ concentrations reached ~0.75 mg-N $L^{-1}$, whereas downstream $NO_3^-$ concentrations were ~0.05 mg-N $L^{-1}$. Between July and November 2015, downstream $NO_3^-$ concentrations exhibited a much lower range (~0.05 to ~0.15 mg-N $L^{-1}$) as compared with upstream (~0.1 to ~0.8 mg-N $L^{-1}$) (Figure 3). This reduction in both magnitude and range of downstream $NO_3^-$ concentrations under baseflow conditions could arise either from dilution of $NO_3^-$, as a result of downstream accretion of water sources with much lower $NO_3^-$ concentrations, or by removal of $NO_3^-$ through biogeochemical processes, necessitating a mass-balance evaluation (see section 3.3).

The widening gap in $NO_3^-$ concentrations between upstream and downstream sites after mid-July 2015 corresponded with a decline in GPP/ER, which fell below 1, indicating a change to net heterotrophy (Figure 4c). During the low-flow period from mid-July to November 2015, Big Creek was heterotrophic for ~90% of days. Daily streamwater $EpCO_2$ doubled between mid-July and November 2015, from 4.5 to 9.1 times atmospheric pressure, independently confirming an increase in rates of respiration ($CO_2$ release), relative to photosynthesis ($CO_2$ uptake).

During the higher-flow period from mid-January to mid-July, Big Creek was predominantly net autotrophic (GPP/ER > 1 for 52% of days). Net heterotrophic conditions prevailed predominantly during lower-flow intervals between storm events, with GPP/ER < 1 typically during and immediately after storm events.

Molar C:N ratios at Carver also increased markedly after mid-July, from ~300 to >800 (Figure 4d). This stoichiometric depletion of N, along with persistence of low $NO_3^-$ concentrations below 0.1 mg-N $L^{-1}$ (falling to <0.04 mg-N $L^{-1}$), suggests that algal growth may have been limited by low N availability at Carver over the late summer and autumn of 2015.

**3.3. Nitrate Reach Mass Balance to Quantify Seasonal Nitrate Removal during Baseflow Conditions.** Mean daily $NO_3^-$ mass balances for the eight seasonal quiescent baseflow periods between February and October 2015 are presented in Table 1. Mean daily $NO_3^-$ input loadings to the reach ($L_T$) increased from 17.3 kg-N $d^{-1}$ in February to 61.7 kg-N $d^{-1}$ in



DOI: 10.1021/acs.est.8b03074
Environ. Sci. Technol. 2018, 52, 13708–13717

Table 2. Seasonal Patterns in Mean Daily $NO_3^-$ Removal Rate ($U_T$) along the 6.5 km Experimental Reach of Big Creek, Under Low-Flow Conditions, And Mean Daily Assimilatory Uptake of $NO_3^-$ by Photoautotrophs ($U_A$)[a]

| season | date range | instream $NO_3^-$ removal rate ($U_T$) (mg-N $L^{-1}$ $d^{-1}$) | assimilatory $NO_3^-$ uptake ($U_A$) (mg-N $L^{-1}$ $d^{-1}$) |
|---|---|---|---|
| winter | 4–13 Feb 2015 | 0.077 (0.006) | 0.212 (0.035) |
| spring 1 | 5–12 Apr 2015 | 0.072 (0.017) | 0.256 (0.050) |
| spring 2 | 24 Apr–5 May 2015 | 0.082 (0.018) | 0.355 (0.067) |
| early summer | 2–10 Jun 2015 | 0.090 (0.014) | 0.269 (0.045) |
| mid summer | 11–21 Jul 2015 | 0.066 (0.030) | 0.259 (0.040) |
| late summer | 7–16 Aug 2015 | 0.284 (0.026) | 0.180 (0.016) |
| autumn 1 | 1–14 Sept 2015 | 0.229 (0.019) | 0.115 (0.038) |
| autumn 2 | 1–11 Oct 2015 | 0.656 (0.029) | 0.076 (0.028) |

[a]Standard deviations are shown in parentheses.

Table 3. Seasonal Patterns in Mean Daily $NO_3^-$ Concentration Gains by Net Nitrification (+) and Losses by Net Denitrification (−) long the Experimental Reach of Big Creek, under Low-Flow Conditions; Mean Daily Values of the Ratio between Gross Primary Production and Ecosystem Respiration (GPP/ER); Excess Partial Pressure of Carbon Dioxide ($EpCO_2$); Dissolved Oxygen (DO); Streamflow; and the Percentage of Groundwater Contribution to Streamflow[a]

| season | date range | net nitrification (+) or denitrification (−) (mg-N $L^{-1}$ $d^{-1}$) | GPP/ER | $EpCO_2$ (× atm. press.) | DO (mg-$O_2$ $L^{-1}$) | flow ($m^3$ $s^{-1}$) | % groundwater |
|---|---|---|---|---|---|---|---|
| winter | 4–13 Feb 2015 | +0.135 (0.032) | 1.14 (0.09) | 2.80 (0.20) | 11.9 (0.49) | 1.15 (0.07) | 66.5 (1.34) |
| spring 1 | 5–12 Apr 2015 | +0.184 (0.039) | 1.06 (0.13) | 3.64 (0.20) | 10.2 (0.33) | 3.10 (0.37) | 58.6 (2.38) |
| spring 2 | 24 Apr -5 May 2015 | +0.273 (0.058) | 1.25 (0.16) | 3.81 (0.59) | 10.3 (0.50) | 2.61 (1.16) | 61.7 (5.79) |
| early summer | 2–10 Jun 2015 | +0.179 (0.044) | 1.34 (0.15) | 4.71 (0.49) | 9.39 (0.42) | 3.30 (1.72) | 58.0 (6.48) |
| mid summer | 11–21 Jul 2015 | +0.193 (0.024) | 1.97 (0.78) | 7.15 (0.46) | 8.98 (0.29) | 2.54 (1.28) | 82.8 (7.21) |
| late summer | 7–16 Aug 2015 | −0.104 (0.032) | 0.78 (0.05) | 10.6 (0.83) | 6.95 (0.35) | 0.23 (0.04) | 98.8 (0.98) |
| autumn 1 | 1–14 Sept 2015 | −0.102 (0.027) | 0.62 (0.10) | 9.85 (1.65) | 6.50 (0.54) | 0.24 (0.06) | 96.6 (1.42) |
| autumn 2 | 1–11 Oct 2015 | −0.592 (0.015) | 0.57 (0.23) | 8.17 (1.50) | 7.85 (0.64) | 0.04 (0.004) | 97.8 (0.64) |

[a]Standard deviations are shown in parentheses.

July, then declined rapidly to 7.56 kg-N $d^{-1}$ in August, which also corresponded with an order of magnitude reduction in baseflow discharge. By October, $L_T$ had fallen to only 2.98 kg-N $d^{-1}$. Instream $NO_3^-$ removal ($L_R$) followed a similar pattern to $L_T$, with highest mean daily instream $NO_3^-$ removal during June (24 kg-N $d^{-1}$), then decreasing during the late summer and autumn, and falling to 2.82 kg-N $d^{-1}$ in October. However, the efficiency of instream $NO_3^-$ removal ($U_E$, i.e., $L_R$ expressed as a percentage of $L_T$) increased markedly during the late summer and autumn, from 32% in July to 74–95% between August and October.

The fluvial mass balance therefore confirmed that the observed downstream reductions in $NO_3^-$ concentrations under baseflow were a result of net instream removal of $NO_3^-$ by biogeochemical processes, rather than a dilution effect.

Although $L_T$ and $L_R$ were greatest during the winter to early summer period, $U_E$ and the instream $NO_3^-$ removal rate ($U_T$) increased dramatically during the low flows of the late summer and autumn; $U_T$ increased from ≤0.09 mg-N $L^{-1}$ $d^{-1}$ (February through July), to >0.2 mg-N $L^{-1}$ $d^{-1}$ in August and September, and 0.66 mg-N $L^{-1}$ $d^{-1}$ in October (Table 2). By autumn 2015, >75% of the $NO_3^-$ inputs were removed by biogeochemical processes (Table 1).

We also assessed the efficiency of $NO_3^-$ removal under the alternative scenario, where the increase in flow along the experimental reach was solely from direct groundwater input (S1.6.2). This made relatively little difference to the $U_E$, which also increased markedly during the late summer and autumn, from 46% in July to 72–94% between August and October (Table SI3). The sensitivity analysis (Tables SI1 and SI3) showed that a 50% increase or decrease in either Left Fork or groundwater $NO_3^-$ concentrations made little difference to these findings: a consistent increase in efficiency of $NO_3^-$ removal was observed after July, with August to October $U_E$ values consistently ∼70–95%.

**3.4. Biogeochemical Controls on Nitrate Delivery: Accounting for Assimilatory Nitrate Uptake to Calculate Net Nitrification and Net Denitrification.** From February to July, assimilatory $NO_3^-$ uptake by photosynthesizing plants ($U_A$) consistently exceeded $U_T$ (Table 2) indicating, first, that assimilation of $NO_3^-$ by photoautotrophs was the dominant process removing $NO_3^-$ from the water column; and second that assimilation was partially balanced by net nitrification $NO_3^-$ gains. In contrast, from August to October, $U_T$ exceeded $U_A$, indicating that heterotrophic $NO_3^-$ removal through direct uptake and denitrification was removing $NO_3^-$ along the reach in late summer and autumn.

Table 3 shows that net nitrification gains to the reach ranged from 0.135 mg-N $L^{-1}$ $d^{-1}$ in February to 0.273 mg-N $L^{-1}$ $d^{-1}$ in April/May. However, after July, a pronounced switch from net nitrification gains to net denitrification losses occurred. During late summer and autumn, denitrification losses of $NO_3^-$ increased from ∼0.100 mg-N $L^{-1}$ $d^{-1}$ in August and September to 0.592 mg-N $L^{-1}$ $d^{-1}$ in October. These estimates were based on using an average periphyton C:N molar ratio of 12 for U.S.A. streams.[35,38] We also evaluated the effects of using an average periphyton molar C:N ratio of 8.6, from research in northern European streams.[17] This increased $U_A$ values by ∼39%, but did not alter our findings of a switch between net nitrification between February and July, to net denitrification from August to October. By changing the C:N stoichiometry from 12 to 8.6, net nitrification ranged from


DOI: 10.1021/acs.est.8b03074
Environ. Sci. Technol. 2018, 52, 13708–13717

+0.218 mg-N $L^{-1}$ $d^{-1}$ in February to +0.414 mg-N $L^{-1}$ $d^{-1}$ in April/May, with net denitrification ranging from −0.033 mg-N $L^{-1}$ $d^{-1}$ in August to −0.562 mg-N $L^{-1}$ $d^{-1}$ in October.

Net nitrification and denitrification rates were compared with mean daily GPP/ER, $EpCO_2$, streamflow and percentage groundwater discharge (Table 3). The shift from net nitrification to net denitrification corresponded directly with (1) a change in stream metabolism from net autotrophic (GPP/ER in July was 1.97) to net heterotrophic (GPP/ER fell below 1, to 0.78 in August, 0.62 in September, and 0.57 in October); and (2) an increase in $EpCO_2$ and a reduction in DO arising from the increases in microbial respiration relative to photosynthesis.

The alternative scenario where flow accretion between Mt Judea and Carver was attributed to direct groundwater discharge to Big Creek also had no effect on the timing of the shift from net nitrification to denitrification (S1.6.2, Table SI4). Sensitivity analysis (Tables SI2 and SI4) also showed that, irrespective of a 50% increase or decrease in either Left Fork or groundwater $NO_3^-$ concentrations, the same consistent switch between net nitrification and net denitrification was observed after July.

The consistency in this observed switch between instream $NO_3^-$ production and instream $NO_3^-$ removal, and its synchronicity with measured changes in stream metabolism, provides compelling evidence that the marked change in instream $NO_3^-$ processing and delivery after July was linked to changes in stream metabolism from net autotrophy to net heterotrophy.

The karst streams of the Ozarks are characterized by a large hyporheic zone,[42,43] a hotspot of nitrogen transformation.[44] Water residence times and redox conditions provide a key control on changes between $NO_3^-$ removal and $NO_3^-$ production with hyporheic zone sediments.[45−48] In Big Creek, the winter to midsummer period was characterized by higher baseflows (at least an order of magnitude greater than late summer/autumn baseflows), and net autotrophy resulting in higher instream DO concentrations. Rapid movement of well-oxygenated water throughout the water column, and into the hyporheic zone, promotes aerobic metabolism of organic matter and release of $NO_3^-$ through nitrification.[46,49] From winter to midsummer, net nitrification was observed in Big Creek, and nitrification in the hyporheic zone may have been responsible for buffering the effects of photosynthetic assimilatory uptake of $NO_3^-$.

Under the more sluggish flow conditions during late summer and autumn, available oxygen is depleted as a result of increased heterotrophic activity. The reduced movement of water and oxygen through the hyporheic zone favors a shift to respiratory pathways with denitrification (conversion of nitrate to $N_2O$ and/or $N_2$ gas).[50,51] Unlike assimilation of $NO_3^-$ into plant biomass, which retains N temporarily, denitrification results in a permanent loss of bioavailable N. The low baseflows of late summer and autumn 2015, resulted in higher water residence times and a greater proportion of flow moving through the hyporheic zone. This provides greater exposure and water contact time with microbial biofilms where denitrification occurs.[51] The death and breakdown of biomass during the late summer and autumn contribute to the availability of organic matter for microbial decomposition, promoting higher rates of microbial respiration relative to photosynthesis, losses of DO, and greater availability of organic carbon as a resource for denitrifying bacteria.[45,52,53] Denitrification within the hyporheic zone may therefore be responsible for losses of $NO_3^-$ in Big Creek during the late summer and autumn. Although denitrification can also occur on suspended sediments within the water column,[54,55] this is likely to be a second order effect under baseflow conditions in a groundwater-fed stream, where suspended solids concentrations are low (typically <5 mg $L^{-1}$).

Under baseflow conditions, instream assimilatory $NO_3^-$ uptake by photosynthesizing plants and hyporheic-zone denitrification along the experimental reach removed between ∼30 and ∼90% of the $NO_3^-$ input load. During the period of monitoring (spring 2014 to spring 2017) $NO_3^-$ loading to the upstream section of Big Creek (at Mt Judea) was attenuated by instream processing such that no CAFO-related impacts on either stream nutrient concentrations or metabolism were discernible at the downstream location (Carver), and thus, to the Buffalo River. Future monitoring will be needed to detect whether long-term changes in nutrients and organic carbon inputs may occur, whether this stimulates higher rates of heterotrophic and/or autotrophic activity, and any longer-term effects on the capacity of assimilation and denitrification processes to remove and buffer any increase in nutrient loadings.

The novelty of this research is the combination of continuous, high-frequency in situ stream metabolism and nitrate measurements, to apportion the net effects of assimilation, nitrification, and denitrification on changes in baseflow nitrate fluxes at the river-reach to watershed scale. In this case, we found that, during winter to midsummer periods, $NO_3^-$ uptake in Big Creek was dominated by assimilation by photoautotrophs, which was partially compensated by release of $NO_3^-$ from nitrification. In late summer, the predominant metabolic pathway switched to net heterotrophy and heterotrophic $NO_3^-$ removal through direct uptake and denitrification became the dominant process of nitrate removal. Removal of $NO_3^-$ by assimilation and denitrification provides an important "self-cleansing" ecosystem service, resulting in a pronounced shift in C:N stoichiometry and decreasing $NO_3^-$ concentrations to low levels which would be expected to limit algal growth.[56]

This approach provides a means of scaling up, from microscale and mesoscale process experiments and measurements, which are, by necessity, short-term and localized, to explore how river nitrate delivery responds to shifts in stream metabolism, from day-to-day and seasonal to interannual variability. This research, and the methods presented here, are applicable along the river continuum, from headwaters to large-scale fluvial systems (with large spatial and temporal variability in nutrient fluxes), and offer a valuable way forward in quantifying net process controls on the fate and transport of nitrogen in fluvial systems.

## ■ ASSOCIATED CONTENT

### Supporting Information

The Supporting Information is available free of charge on the ACS Publications website at DOI: 10.1021/acs.est.8b03074.

S1, Methods: Land use and cover data; site hydrogeology; high-frequency water-quality monitoring; streamflow measurement; hydrograph separation; analysis of diurnal dissolved oxygen curves to calculate primary production and respiration; calculation of DIC and $EpCO_2$; nitrate mass-balance calculations; and S2,



DOI: 10.1021/acs.est.8b03074
Environ. Sci. Technol. 2018, 52, 13708−13717

Results: Figure SI1 time series of nitrate and flow and nitrate plotted against stream flow for Mt Judea; Tables SI1 and SI2, sensitivity analysis based on estimates of $NO_3^-$ load inputs from Left Fork; Tables SI3 and SI4, alternative scenario sensitivity analysis based on estimates of $NO_3^-$ load inputs from groundwater; and additional references (PDF)

## AUTHOR INFORMATION


### Corresponding Author

*E-mail: hpj@ceh.ac.uk.

### ORCID

Helen P. Jarvie: 0000-0002-4984-1607

Phillip D. Hays: 0000-0001-5491-9272


### Notes

The authors declare no competing financial interest.

## ACKNOWLEDGMENTS

H.P.J. and R.J.W. were supported by NERC National Capability projects NEC05966 and NEC04879. Funding for the Big Creek Research and Extension monitoring was provided by the Arkansas Governor's Office and State Legislature to the University of Arkansas System's Division of Agriculture. Hydrological and chemical monitoring by the USGS were supported by a National Park Service/USGS Water Quality Partnership Grant, administered by the USGS. Any use of trade, firm, or product names is for descriptive purposes only and does not imply endorsement by the U.S. Government.

## REFERENCES


(1) Smith, V. H. Eutrophication of freshwater and coastal marine ecosystems - A global problem. *Environ. Sci. Pollut. Res.* **2003**, *10* (2), 126−139.

(2) Dodds, W. K.; Bouska, W. W.; Eitzmann, J. L.; Pilger, T. J.; Pitts, K. L.; Riley, A. J.; Schloesser, J. T.; Thornbrugh, D. J. Eutrophication of US Freshwaters: Analysis of Potential Economic Damages. *Environ. Sci. Technol.* **2009**, *43* (1), 12−19.

(3) Dodds, W. K.; Smith, V. H. Nitrogen, phosphorus, and eutrophication in streams. *Inland Waters* **2016**, *6* (2), 155−164.

(4) Peterson, B. J.; Wollheim, W. M.; Mulholland, P. J.; Webster, J. R.; Meyer, J. L.; Tank, J. L.; Marti, E.; Bowden, W. B.; Valett, H. M.; Hershey, A. E.; McDowell, W. H.; Dodds, W. K.; Hamilton, S. K.; Gregory, S.; Morrall, D. D. Control of nitrogen export from watersheds by headwater streams. *Science* **2001**, *292* (5514), 86−90.

(5) Alexander, R. B.; Boyer, E. W.; Smith, R. A.; Schwarz, G. E.; Moore, R. B. The role of headwater streams in downstream water quality. *J. Am. Water Resour. Assoc.* **2007**, *43* (1), 41−59.

(6) Jarvie, H. P.; Sharpley, A. N.; Scott, J. T.; Haggard, B. E.; Bowes, M. J.; Massey, L. B. Within-River Phosphorus Retention: Accounting for a Missing Piece in the Watershed Phosphorus Puzzle. *Environ. Sci. Technol.* **2012**, *46* (24), 13284−13292.

(7) Mulholland, P. J.; Helton, A. M.; Poole, G. C.; Hall, R. O.; Hamilton, S. K.; Peterson, B. J.; Tank, J. L.; Ashkenas, L. R.; Cooper, L. W.; Dahm, C. N.; Dodds, W. K.; Findlay, S. E. G.; Gregory, S. V.; Grimm, N. B.; Johnson, S. L.; McDowell, W. H.; Meyer, J. L.; Valett, H. M.; Webster, J. R.; Arango, C. P.; Beaulieu, J. J.; Bernot, M. J.; Burgin, A. J.; Crenshaw, C. L.; Johnson, L. T.; Niederlehner, B. R.; O'Brien, J. M.; Potter, J. D.; Sheibley, R. W.; Sobota, D. J.; Thomas, S. M. Stream denitrification across biomes and its response to anthropogenic nitrate loading. *Nature* **2008**, *452* (7184), 202−U46.

(8) Mulholland, P. J.; Valett, H. M.; Webster, J. R.; Thomas, S. A.; Cooper, L. W.; Hamilton, S. K.; Peterson, B. J. Stream denitrification and total nitrate uptake rates measured using a field N-15 tracer addition approach. *Limnol. Oceanogr.* **2004**, *49* (3), 809−820.

(9) Tank, J. L.; Marti, E.; Riis, T.; von Schiller, D.; Reisinger, A. J.; Dodds, W. K.; Whiles, M. R.; Ashkenas, L. R.; Bowden, W. B.; Collins, S. M.; Crenshaw, C. L.; Crowl, T. A.; Griffiths, N. A.; Grimm, N. B.; Hamilton, S. K.; Johnson, S. L.; McDowell, W. H.; Norman, B. M.; Rosi, E. J.; Simon, K. S.; Thomas, S. A.; Webster, J. R. Partitioning assimilatory nitrogen uptake in streams: an analysis of stable isotope tracer additions across continents. *Ecol. Monogr.* **2018**, *88* (1), 120−138.

(10) Tank, J. L.; Meyer, J. L.; Sanzone, D. M.; Mulholland, P. J.; Webster, J. R.; Peterson, B. J.; Wollheim, W. M.; Leonard, N. E. Analysis of nitrogen cycling in a forest stream during autumn using a N-15-tracer addition. *Limnol. Oceanogr.* **2000**, *45* (5), 1013−1029.

(11) Ensign, S. H.; Doyle, M. W. Nutrient spiraling in streams and river networks. *Journal of Geophysical Research-Biogeosciences* **2006**, *111* (G4), G04009.

(12) Rode, M.; Halbedel nee Angelstein, S.; Anis, M. R.; Borchardt, D.; Weitere, M. Continuous in-stream assimilatory nitrate uptake from high frequency sensor measurements. *Environ. Sci. Technol.* **2016**, *50* (11), 5685−5694.

(13) Bowes, M. J.; Jarvie, H. P.; Halliday, S. J.; Skeffington, R. A.; Wade, A. J.; Loewenthal, M.; Gozzard, E.; Newman, J. R.; Palmer-Felgate, E. J. Characterising phosphorus and nitrate inputs to a rural river using high-frequency concentration-flow relationships. *Sci. Total Environ.* **2015**, *511*, 608−620.

(14) Halliday, S. J.; Skeffington, R. A.; Wade, A. J.; Bowes, M. J.; Gozzard, E.; Newman, J. R.; Loewenthal, M.; Palmer-Felgate, E. J.; Jarvie, H. P. High-frequency water quality monitoring in an urban catchment: hydrochemical dynamics, primary production and implications for the Water Framework Directive. *Hydrological Processes* **2015**, *29* (15), 3388−3407.

(15) Halliday, S. J.; Skeffington, R. A.; Wade, A. J.; Bowes, M. J.; Read, D. S.; Jarvie, H. P.; Loewenthal, M. Riparian shading controls instream spring phytoplankton and benthic algal growth. *Environmental Science-Processes & Impacts* **2016**, *18* (6), 677−689.

(16) Wade, A. J.; Palmer-Felgate, E. J.; Halliday, S. J.; Skeffington, R. A.; Loewenthal, M.; Jarvie, H. P.; Bowes, M. J.; Greenway, G. M.; Haswell, S. J.; Bell, I. M.; Joly, E.; Fallatah, A.; Neal, C.; Williams, R. J.; Gozzard, E.; Newman, J. R. Hydrochemical processes in lowland rivers: insights from in situ, high-resolution monitoring. *Hydrol. Earth Syst. Sci.* **2012**, *16* (11), 4323−4342.

(17) Rode, M.; Wade, A. J.; Cohen, M. J.; Hensley, R. T.; Bowes, M. J.; Kirchner, J. W.; Arhonditsis, G. B.; Jordan, P.; Kronvang, B.; Halliday, S. J.; Skeffington, R. A.; Rozemeijer, J. C.; Aubert, A. H.; Rinke, K.; Jomaa, S. Sensors in the stream: The High-frequency wave of the present. *Environ. Sci. Technol.* **2016**, *50* (19), 10297−10307.

(18) Cohen, M. J.; Kurz, M. J.; Heffernan, J. B.; Martin, J. B.; Douglass, R. L.; Foster, C. R.; Thomas, R. G. Diel phosphorus variation and the stoichiometry of ecosystem metabolism in a large spring-fed river. *Ecol. Monogr.* **2013**, *83* (2), 155−176.

(19) Hensley, R. T.; Cohen, M. J. On the emergence of diel solute signals in flowing waters. *Water Resour. Res.* **2016**, *52* (2), 759−772.

(20) Hensley, R. T.; Cohen, M. J.; Korhnak, L. V. Inferring nitrogen removal in large rivers from high-resolution longitudinal profiling. *Limnol. Oceanogr.* **2014**, *59* (4), 1152−1170.

(21) Kunz, J. V.; Hensley, R.; Brase, L.; Borchardt, D.; Rode, M. High frequency measurements of reach scale nitrogen uptake in a fourth order river with contrasting hydromorphology and variable water chemistry (Weisse Elster, Germany). *Water Resour. Res.* **2017**, *53* (1), 328−343.

(22) Kraus, T. E. C.; O'Donnell, K.; Downing, B. D.; Burau, J. R.; Bergamaschi, B. A. Using paired in situ high frequency nitrate measurements to better understand controls on nitrate concentrations and estimate nitrification rates in a wastewater-impacted river. *Water Resour. Res.* **2017**, *53* (10), 8423−8442.

(23) Jones, C.; Kim, S. W.; Schilling, K. Use of continuous monitoring to assess stream nitrate flux and transformation patterns. *Environ. Monit. Assess.* **2017**, *189*, 35.

(24) Wollheim, W. M.; Mulukutla, G. K.; Cook, C.; Carey, R. O. Aquatic nitrate retention at river network scales across flow conditions




DOI: 10.1021/acs.est.8b03074
*Environ. Sci. Technol.* 2018, 52, 13708−13717

determined using nested in situ sensors. *Water Resour. Res.* **2017**, *53* (11), 9740−9756.
(25) Jarvie, H. P.; Sharpley, A. N.; Brahana, V.; Simmons, T.; Price, A.; Neal, C.; Lawlor, A. J.; Sleep, D.; Thacker, S.; Haggard, B. E. Phosphorus retention and remobilization along hydrological pathways in karst terrain. *Environ. Sci. Technol.* **2014**, *48* (9), 4860−4868.
(26) American Public Health Association (APHA). Alkalinity: Titration Method 2320 B. In *Standard Methods for the Examination of Water and Wastewater*, 23rd ed. 1987. ISBN: 978−0-87553−287−5.
(27) Rantz, S. E. Measurement and computation of streamflow: Vol. 1, Measurement of stage and discharge. In *U.S. Geological Survey*, Water Supply Paper 2175. 1982.
(28) Jarvie, H. P.; Neal, C.; Smart, R.; Owen, R.; Fraser, D.; Forbes, I.; Wade, A. Use of continuous water quality records for hydrograph separation and to assess short-term variability and extremes in acidity and dissolved carbon dioxide for the River Dee, Scotland. *Sci. Total Environ.* **2001**, *265* (1−3), 85−98.
(29) O'Connor, D. J.; Ditoro, D. M. Photosynthesis and oxygen balance in streams. *Journal of the Sanitary Engineering Division. Proceedings of the American Society of Civil Engineers* **1970**, *96* (2), 547−571.
(30) Williams, R. J.; White, C.; Harrow, M. L.; Neal, C. Temporal and small-scale spatial variations of dissolved oxygen in the Rivers Thames, Pang and Kennet, UK. *Sci. Total Environ.* **2000**, *251*, 497−510.
(31) Chapra, S. C.; Ditoro, D. M. Delta method for estimating primary production, respiration, and reaeration in streams. *J. Environ. Eng.* **1991**, *117* (5), 640−655.
(32) Bernhardt, E. S.; Heffernan, J. B.; Grimm, N. B.; Stanley, E. H.; Harvey, J. W.; Arroita, M.; Appling, A. P.; Cohen, M. J.; McDowell, W. H.; Hall, R. O.; Read, J. S.; Roberts, B. J.; Stets, E. G.; Yackulic, C. B. The metabolic regimes of flowing waters. *Limnol. Oceanogr.* **2018**, *63*, S99−S118.
(33) Odum, H. T. Primary production in flowing waters. *Limnol. Oceanogr.* **1956**, *1*, 102−117.
(34) Jarvie, H. P.; King, S. M.; Neal, C. Inorganic carbon dominates total dissolved carbon concentrations and fluxes in British rivers: Application of the THINCARB model - Thermodynamic modelling of inorganic carbon in freshwaters. *Sci. Total Environ.* **2017**, *575*, 496−512.
(35) King, S. A.; Heffernan, J. B.; Cohen, M. J. Nutrient flux, uptake, and autotrophic limitation in streams and rivers. *Freshwater Science* **2014**, *33* (1), 85−98.
(36) Hall, R. O.; Tank, J. L. Ecosystem metabolism controls nitrogen uptake in streams in Grand Teton National Park, Wyoming. *Limnol. Oceanogr.* **2003**, *48* (3), 1120−1128.
(37) Hall, R. O.; Beaulieu, J. J. Estimating autotrophic respiration in streams using daily metabolism data. *Freshwater Science* **2013**, *32* (2), 507−516.
(38) Stelzer, R. S.; Lamberti, G. A. Effects of N: P ratio and total nutrient concentration on stream periphyton community structure, biomass, and elemental composition. *Limnol. Oceanogr.* **2001**, *46* (2), 356−367.
(39) Redfield, A. C. The biological control of chemical factors in the environment. *American Scientist* **1958**, *46* (3), 205−221.
(40) Evans-White, M. A.; Haggard, B. E.; Scott, J. T. A Review of stream nutrient criteria development in the United States. *Journal of Environmental Quality* **2013**, *42* (4), 1002−1014.
(41) Sharpley, A. N.; Haggard, B. E.; Berry, L.; Brye, K.; Burke, J.; Daniels, M. B.; Gbur, E.; Glover, T.; Hays, P.; Kresse, T.; VanDevender, K. W. Nutrient concentrations in Big Creek correlate to regional watershed land use. *Agricultural & Environmental Letters* **2017**, *2*, 170027.
(42) Miller, R. B.; Heeren, D. M.; Fox, G. A.; Halihan, T.; Storm, D. E.; Mittelstet, A. R. The hydraulic conductivity structure of gravel-dominated vadose zones within alluvial floodplains. *J. Hydrol.* **2014**, *513*, 229−240.
(43) Miller, R. B.; Heeren, D. M.; Fox, G. A.; Halihan, T.; Storm, D. E. Heterogeneity influences on stream water-groundwater interactions in a gravel-dominated floodplain. *Hydrol. Sci. J.* **2016**, *61* (4), 741−750.
(44) Triska, F. J.; Duff, J. H.; Avanzino, R. J. The role of water exchange between a stream and its hyporheic zone in nitrogen cycling at the terrestrial aquatic interface. *Hydrobiologia* **1993**, *251* (1−3), 167−184.
(45) Zarnetske, J. P.; Haggerty, R.; Wondzell, S. M.; Baker, M. A. Labile dissolved organic carbon supply limits hyporheic denitrification. *J. Geophys. Res.* **2011**, *116*, G04036.
(46) Zarnetske, J. P.; Haggerty, R.; Wondzell, S. M.; Bokil, V. A.; Gonzalez-Pinzon, R. Coupled transport and reaction kinetics control the nitrate source-sink function of hyporheic zones. *Water Resour. Res.* **2012**, *48*, W11508.
(47) Harvey, J. W.; Bohlke, J. K.; Voytek, M. A.; Scott, D.; Tobias, C. R. Hyporheic zone denitrification: Controls on effective reaction depth and contribution to whole-stream mass balance. *Water Resour. Res.* **2013**, *49* (10), 6298−6316.
(48) Moatar, F.; Abbott, B. W.; Minaudo, C.; Curie, F.; Pinay, G. Elemental properties, hydrology, and biology interact to shape concentration discharge curves for carbon, nutrients, sediment, and major ions. *Water Resour. Res.* **2017**, *53* (2), 1270−1287.
(49) Zarnetske, J. P.; Haggerty, R.; Wondzell, S. M.; Baker, M. A. Dynamics of nitrate production and removal as a function of residence time in the hyporheic zone. *J. Geophys. Res.* **2011**, *116*, G01025.
(50) Zarnetske, J. P.; Haggerty, R.; Wondzell, S. M. Coupling multiscale observations to evaluate hyporheic nitrate removal at the reach scale. *Freshwater Science* **2015**, *34* (1), 172−186.
(51) Palmer-Felgate, E. J.; Mortimer, R. J. G.; Krom, M. D.; Jarvie, H. P. Impact of point-source pollution on phosphorus and nitrogen cycling in stream-bed sediments. *Environ. Sci. Technol.* **2010**, *44* (3), 908−914.
(52) Aubert, A. H.; Breuer, L. New seasonal shift in in-stream diurnal nitrate cycles identified by mining high-frequency data. *PLoS One* **2016**, *11*, (4); e0153138.
(53) Dodds, W. K.; Marti, E.; Tank, J. L.; Pontius, J.; Hamilton, S. K.; Grimm, N. B.; Bowden, W. B.; McDowell, W. H.; Peterson, B. J.; Valett, H. M.; Webster, J. R.; Gregory, S. Carbon and nitrogen stoichiometry and nitrogen cycling rates in streams. *Oecologia* **2004**, *140* (3), 458−467.
(54) Liu, T.; Xia, X. H.; Liu, S. D.; Mou, X. L.; Qiu, Y. W. Acceleration of Denitrification in Turbid Rivers Due to Denitrification Occurring on Suspended Sediment in Oxic Waters. *Environ. Sci. Technol.* **2013**, *47* (9), 4053−4061.
(55) Xia, X. H.; Jia, Z. M.; Liu, T.; Zhang, S. B.; Zhang, L. W. Coupled Nitrification-Denitrification Caused by Suspended Sediment (SPS) in Rivers: Importance of SPS Size and Composition. *Environ. Sci. Technol.* **2017**, *51* (1), 212−221.
(56) Jarvie, H. P.; Smith, D. R.; Norton, L. R.; Edwards, F.; Bowes, M. J.; King, S. M.; Scarlett, P.; Davies, S.; Dils, R.; Bachiller-Jareno, N. Phosphorus and Nitrogen Limitation and Impairment of Headwater Streams Relative to Rivers in Great Britain: A National Perspective on Eutrophication. *Sci. Total Environ.* **2018**, *621*, 849−862.


DOI: 10.1021/acs.est.8b03074
*Environ. Sci. Technol.* 2018, 52, 13708−13717